ELSEVIER

Advances in Colloid and Interface Science
96 (2002) 143–167

ADVANCES IN COLLOID AND INTERFACE SCIENCE

www.elsevier.com/locate/cis

Capillary condensation as a morphological transition

Konstantin G. Kornev[a], Inna K. Shingareva[b], Alexander V. Neimark[a,*]

[a] *Center for Modeling and Characterization of Nanoporous Materials, TRI / Princeton, 601 Prospect Avenue, Princeton, NJ 08542-0625, USA*
[b] *Departamento de Matematicas, Universidad de Sonora, 83000 Hermosillo, Sonora, Mexico*

Abstract

The process of capillary condensation/evaporation in cylindrical pores is considered within the idea of symmetry breaking. Capillary condensation/evaporation is treated as a morphological transition between the wetting film configurations of different symmetry. We considered two models: (i) the classical Laplace theory of capillarity and (ii) the Derjaguin model which takes into account the surface forces expressed in terms of the disjoining pressure. Following the idea of Everett and Haynes, the problem of condensation/evaporation is considered as a transition from bumps/undulations to lenses. Using the method of phase portraits, we discuss the mathematical mechanisms of this transition hidden in the Laplace and Derjaguin equations. Analyzing the energetic barriers of the bump and lens formation, it is shown that the bump formation is a prerogative of capillary condensation: for the vapor–liquid transition in a pore, the bump plays the same role as the spherical nucleus in a bulk fluid. We show also that the Derjaguin model admits a variety of interfacial configurations responsible for film patterning at specific conditions.

Keywords: Capillary condensation/evaporation; Interfacial configurations; Bump formation; Film patterning

* Corresponding author. Tel.: +1-609-430-4818; fax: +1-609-683-7149.
E-mail address: aneimark@triprinceton.org (A.V. Neimark).

0001-8686/02/$ - see front matter
PII: S0001-8686(01)00079-3

Contents

1. Introduction

This paper is devoted to the 80th anniversary of Nikolai Vladimirovich Churaev, who has set a tone in the science of colloids and interfaces for over almost 60 years of his carrier. Among his seminal works, the papers on capillary condensation phenomenon and associated problems of stability of wetting films deserve a special attention [1–4]. These papers show that the concept of disjoining pressure provides us with a rational to catch the microphysics of wetting films within a macroscopic approach.

The hysteretic character of the capillary condensation phenomenon is its characteristic property. It is well documented in numerous experiments that the process of capillary condensation and the reverse process of evaporation follow different pathways on the phase diagram so that the adsorption–desorption isotherm forms a prominent hysteretic loop [5–10]. The hysteretic character of the adsorption/desorption process has been explained by Derjaguin more then 60 years ago by the interplay between capillary and surface (adhesion) forces [11]. This concept has later been elaborated in a series of papers summarized by Derjaguin and Churaev in their comprehensive monograph [3], and also in different terms by Broekhoff and de Boer [5–7], and Saam and Cole [12]. In these papers, the process of capillary condensation is treated as the growth of a uniform adsorption film coating the pore walls up to the limit of its stability followed by the spontaneous pore filling due to irreversible condensation. Therewith, the conditions of film instability differ significantly from the conditions of phase equilibrium between the adsorption film and the meniscus of condensed fluid that gives rise to the observed

hysteretic behavior in capillary condensation and desorption. The qualitative predictions of the Derjaguin theory have been confirmed by the density functional theory and molecular simulations [13–15]. Although this scenario of capillary condensation allows one to determine the conditions of equilibrium and stability of adsorption films, the pathway of phase transformations is left aside. There are two potential mechanisms of phase transformations in real systems: nucleation and spinodal decomposition [16,17]. While nucleation is related to a localized density fluctuation in a metastable phase, spinodal decomposition assumes that the phase transition happens via spatially oscillating fluctuations in a thermodynamically unstable phase [16,17], in particular, in unstable free and deposited liquid films [18–21]. Nucleation in slit-shaped pores has recently enjoyed a lot of attention. A liquid bridge as a nucleus of capillary condensation in a slit-shaped pore was analyzed analytically by Restagno et al. [22] and Talanquer and Oxtoby [23]. While the former authors employed a simple approximate model to access the free energy barrier of nucleation, the latter used a two-dimensional local density functional theory in the gradient approximation. The processes of formation and snap-off of liquid bridges and the reverse processes of cavitation, or bubble formation, within narrow gaps were simulated by molecular dynamics and Monte Carlo methods [24–29]. Relevant lattice and off-lattice simulations of liquid–liquid separation in pores, including spinodal decomposition were performed in slit-shaped and cylindrical pores [30–36]. Gelb and Gubbins [37–39] performed MD simulations of spinodal decomposition of a symmetric LJ mixture in a cylindrical pore. As the system considered in this paper is related to the capillary condensation in a cylindrical pore, we can refer only to a seminal paper of Everett and Haynes [40], who considered the mechanism of capillary condensation in a cylindrical pore based on the Laplace theory of capillarity without taking into account fluid–solid interactions. They put forward an idea that the nucleation of the liquid phase within a capillary proceeds via the formation of an unduloidal liquid bump which then spontaneously transforms into a liquid bridge spanning the pore.

1.1. Paper outline

In this paper, we apply the Derjaguin approach to analyze the interactions between the capillary and surface forces focusing on the formation of symmetry breaking configurations which serve as nuclei for phase transformations. In so doing, we reformulate the problem of capillary condensation/evaporation as a problem of a morphological transition between the translation invariant configurations of equilibrium wetting films and menisci. We apply the method of dynamic systems to classify the equilibrium configurations of interfaces permitted by the Derjaguin equation. These configurations include: (a) stable, metastable and unstable uniform films; (b) menisci of liquid drops, liquid bridges/lenses, and lamellae; (c) bubbles; (d) solitary bumps/indentations on uniform films; and (e) periodically undulating films. The phase portraits show possible pathways of the phase transformations between configurations of different symmetry. We show that the transition from a translation invariant uniform metastable wetting film to a

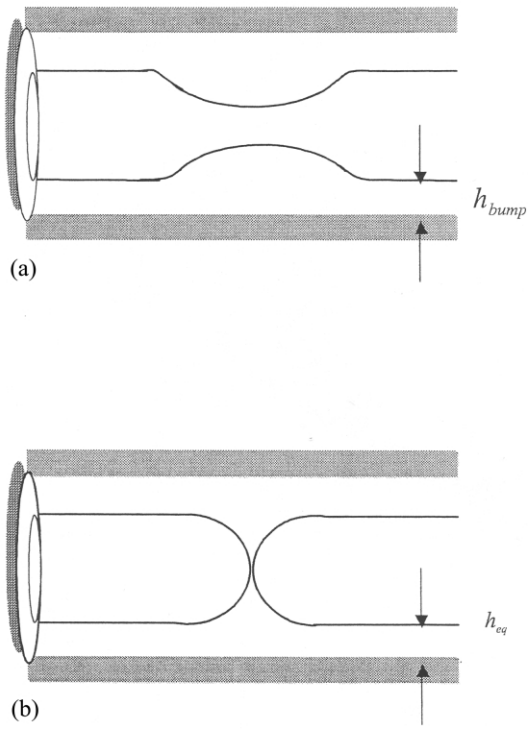

Fig. 1. Bump — lens transformation.

stable meniscus occurs via the nucleation of a solitary bump, which has a lower free energy barrier than a liquid lens/bridge. This scenario is similar to that considered by Everett and Haynes [40]; their account for the surface forces allows us to trace a continuous path from the growing adsorption film to the growing bump to the liquid lens bridging the pore (Fig. 1).

The paper is organized as follows. In Section 2, we start from a brief review of the Derjaguin model of capillarity as related to equilibrium and stability of wetting films, condensation and desorption in a cylindrical pore. Then we discuss the foundations of metastability, spinodals, and hysteresis observed during capillary condensation/evaporation cycles. In Section 3, we introduce the method of phase portraits and consider the macroscopic films, for which the surface/adhesion forces are insignificant and equilibrium configurations are determined by the Laplace equation [41]. We revisit the analysis performed earlier by Everett and Haynes [40] to demonstrate how the method of phase portraits works. In particular, we show the nodoidal and unduloidal solutions [40–45] as they are viewed within the framework of the general theory of dynamic systems. Then we consider morphological transitions in macroscopic films. A sequence of transformations from unduloidal to nodoidal films is traced to reveal the mechanism of symmetry

breaking in this system. The solution corresponding to a solitary bump is discussed in detail.

In Section 4, we apply the phase portrait method to the Derjaguin equation and study equilibrium configurations of wetting films of van der Waals' like fluids. The disjoining pressure isotherms of these films are usually modeled by monotonous dependencies of the forms $\Pi \propto 1/h^{\eta}$, $\eta > 0$ and $\Pi \propto -\ln h$. Traditionally, the Derjaguin equation has been either applied for description of interface configurations transiting to a uniform film [1–3,5–7,9,11,12,46] or, when discussing the configurations of droplets with finite volume, the linearized capillary term has been used [47–50]; for a comprehensive review see Starov [51]. The phase portrait method is aimed at specification of the film configurations when all the non-linear terms are kept. We show that the topological structure of the phase portraits differs qualitatively from the Laplacian model considered in Section 3. The undulating films enrich classification of solutions to the Derjaguin equation proposed earlier for planar substrates [52]. Special attention is paid to analyses of the film profile behavior when the interface touches the capillary wall. The model validity at the immediate vicinity of the substrate has been checked in a series of publications [51–57]. It has been shown that the results obtained by using the linearized capillary term [46] are questionable. In particular, the solutions are incompatible with the thermodynamic constraint, which demand the finiteness of the integral $\int_0^{\infty} \Pi dh$ [51,54–56]. As is known, the linearized version of the model is unable to reproduce the correct form of boundary condition at the droplet edge or the generalized Young–Laplace equation [51,55,56]. We show that, within the non-linear model, the curve describing the edge of the Hamaker–Lifshitz films cannot be continued to the substrate. The film profile is 'hung up' at a certain microscopic height above the wall. The physical reason is that the capillary forces are unable to compete with the adhesion ones when the film thickness diminishes. The profiles of films with integrable disjoining pressure isotherms suitable from a thermodynamic point of view, for example of the forms $\Pi \propto 1/h^{\eta}$, $0 < \eta < 1$ and $\Pi \propto -\ln h$, can be continued to the substrate surface. However, the price paid for the disjoining pressure monotonicity is the presence of microscopic contact angles. The microscopic contact angles cannot be eliminated, i.e. there are no edges smoothly meeting the capillary wall at the zeroth microscopic contact angle.

In Section 5, we focus on the problem of nucleation and consider a solitary bump on an equilibrium uniform film. The method of phase portraits allows us to assert that the equilibrium bump coexists with the uniform film only in the region of film metastability. The bump evolves into the lens bridging the pore at the conditions corresponding to film/meniscus equilibrium coexistence. The free energy of bump formation decreases as the film thickens and vanished at the spinodal representing the true limit of film stability. In the vicinity of the spinodal, bumps appear due to thermal excitations, while the energy needed for the lens creation is always of the order of σR^2 [9–12,22,23]. Since the work of the bump formation is smaller than that of a lens, a solitary bump rather than a lens represents the nucleus for

capillary condensation. The results of the present study and perspectives for further developments are outlined in Section 6.

Our analysis is restricted to one component fluids. The existence of an inert gas would lead to an additional degree of freedom and the thermodynamic considerations should be augmented accordingly. The condensation from a mixture is beyond the scope of this paper. Also, we do not consider here the spinodal decomposition of an unstable film deposited on the internal surface of a capillary. This phenomenon will be presented elsewhere.

2. Capillary condensation / evaporation in a cylindrical pore within the Derjaguin model

Within this model, the capillary condensation in a cylindrical pore occurs via the continuous growth of a uniform film. The film equilibrium implies a balance of the Laplacian capillary pressure and disjoining pressure $\Pi(h)$ caused by intermolecular forces, see schematic in Fig. 2a. For equilibrium cylindrical films the Derjaguin equation reads as [11]:

$$\left[\frac{\sigma}{(R-h)} + \Pi(h)\right] = P_v - P_l = P_c, \tag{1}$$

where R is the pore radius, σ is the surface tension, and the capillary pressure P_c is the difference between the vapor P_v and liquid P_l pressures. Due to the Kelvin relation, the capillary pressure is expressed via the vapor pressure as $P_c = (kT/v)\ln(P_0/P_v)$, where k is the Boltzmann constant, T is the temperature, v is the molecular volume, and P_0 is the saturation pressure for planar vapor/liquid interface.

The hysteretic character of the condensation/evaporation process is schematically shown in Fig. 2b for van der Waals-like fluids, $\Pi(h) \propto 1/h^{\eta}$, where $\eta = 3$. As we increase the vapor pressure, the film grows following the branch AC. The turnover corresponds to the point C, spinodal separates the regions of stability and instability of the film interface. Above the thickness $h = h_{sc}$, the capillary forces overcome the adhesion ones. Mathematically, the stability condition for vapor–film coexistence is obtained as [2]:

$$\frac{d}{dh}\left[\frac{\sigma}{(R-h)} + \Pi(h)\right] \le 0, \text{ or } \Delta = 1 + \frac{(R-h)^2\Pi'(h)}{\sigma} \le 0. \tag{2}$$

When the thermodynamic stability factor Δ becomes positive, the fluctuations begin to grow explosively. In accordance with Eq. (2), the right U-branch CF in Fig. 2b is thermodynamically unstable. These unstable films on the branch CF could not be realized at equilibrium conditions. Therefore, the uniform film grows along the path ABC up to the spinodal point C where the condensation and pore filling

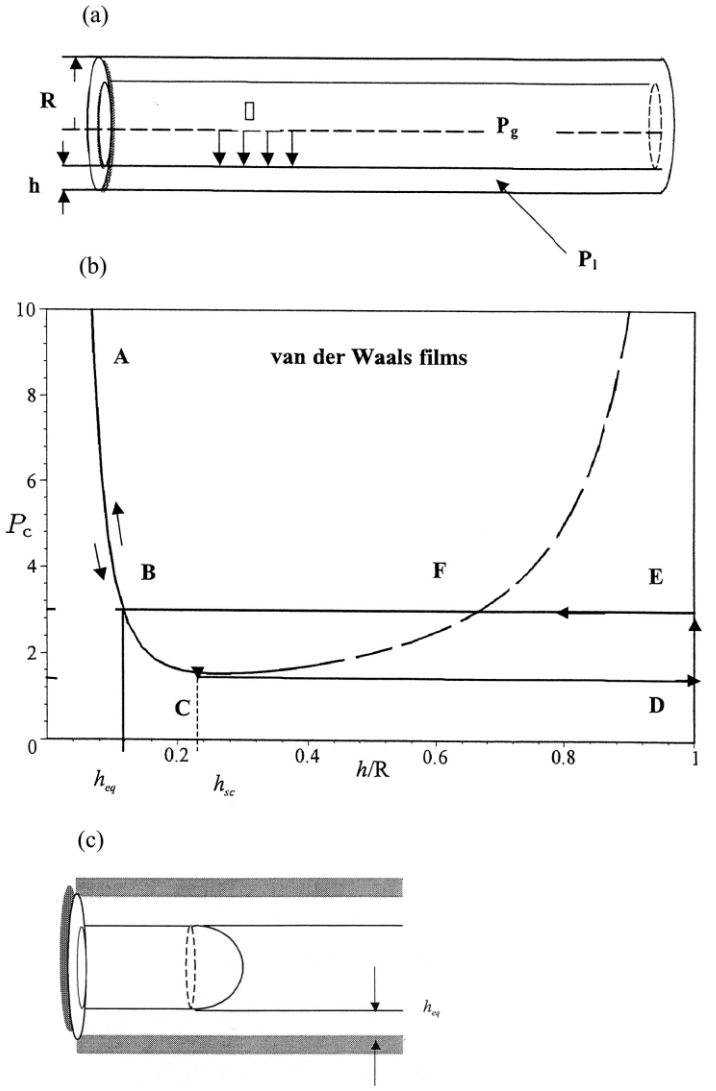

Fig. 2. (a) The film model of adsorption/desorption. (b) For van Waal's films the adsorption path is ABCD, while the desorption follows DEBA–branch. The films at CF–branch cannot be realized. (c) Schematic of meniscus coexisting with the equilibrium film.

occur spontaneously (line CD). The critical thickness $h = h_{sc}$ and the pressure, P_{sc}, are determined from the condition $\Delta = 0$.

In the process of desorption, there exists a thermodynamically equilibrium pathway in which the vapor thread coexists with the meniscus separating the filled and unfilled regions of the capillary [5–11]. The condition for equilibrium coexistence of the vapor and liquid phases is expressed via the Maxwell rule of equal

areas. Denoting the capillary pressure on the line BE by P_{eq}, the Maxwell rule is written as:

$$\Delta\Omega = -2\pi\int_{h_{eq}}^{R}(R-h)(P_{eq}-P_c)dh = 0,$$

or, using Eq. (1) we have:

$$\Delta\Omega = 2\pi\sigma(R-h_{eq}) - \pi P_{eq}(R-h_{eq})^2 + \int_{h_{eq}}^{R}(R-h)\Pi(h)dh = 0. \tag{3}$$

Here, h_{eq} is the thickness of the film left at the capillary wall after evaporation. The first term in Eq. (3) is the film surface energy, the second is the work done to fill the thread of radius $R-h_{eq}$ by vapor, and the third term is the work done by the adhesion forces. Besides Eq. (3), another equilibrium condition, Eq. (1), has to be satisfied on the line BE. Written for the thickness h_{eq} it reads:

$$P_{eq} = P_c(h_{eq}) = \frac{\sigma}{R-h_{eq}} + \Pi(h_{eq}). \tag{4}$$

Combining the condensation and evaporation processes, we get a hysteretic loop ABCDEBA.

As seen, this scenario of capillary condensation and equilibrium vapor/liquid coexistence deals only with the uniform films and the equilibrium meniscus. An analytical expression for the profile of the film transiting to the equilibrium meniscus was obtained in [5–7,11,12,58,59]. However, the theory left beyond its scope the mechanism and a pathway of the film bridging.

3. Morphological transitions in the macroscopic films

Let us first consider the film bridging mechanisms within the framework of the Laplacian capillarity without accounting for the disjoining pressure effects. Discussing the problem of bridging, Everett and Haynes [40] used the explicit form of the solution of the Laplace equation [41–45]. Here, we focus on the mathematical mechanism of bridging hidden in the Laplace equation.

Applied to the axisymmetric interfaces, the Laplace equation for the film thickness profile $h(z)$, z is the axial coordinate, takes the form:

$$P_c = \frac{\sigma h''}{(1+h'^2)^{3/2}} + \frac{\sigma}{(R-h)(1+h'^2)^{1/2}}. \tag{5}$$

It is well known [40–45] that, except the trivial solutions corresponding to cylindrical and spherical interfaces, Eq. (5) has two classes of periodic solutions, nodoids and unduloids. Nodoids describe the waves with cusped crests where $\mathrm{d}h/\mathrm{d}z \to \infty$.

Unduloids are regular periodic solutions of Eq. (5). In application to capillary condensation phenomenon, three trivial solutions serve as reference points. These are the uniform cylindrical film, the semispherical meniscus associated with the capillary pressure $P_c = 2\sigma/R$, and the spherical bubble corresponding to capillary pressures greater than $P_c \geq 2\sigma/R$. The listed solutions are the limiting cases of nodoids and unduloids. When considering transformations of a cylindrical film with $P_c > \sigma/R$ into a meniscus or a bubble train ($P_c \geq 2\sigma/R$) whose configurations are constructed by using the trivial solutions, one can expect that the film runs over nodoids and unduloids or their fragments. For selection of solutions relevant to capillary condensation/evaporation, we apply the methods of dynamic systems.

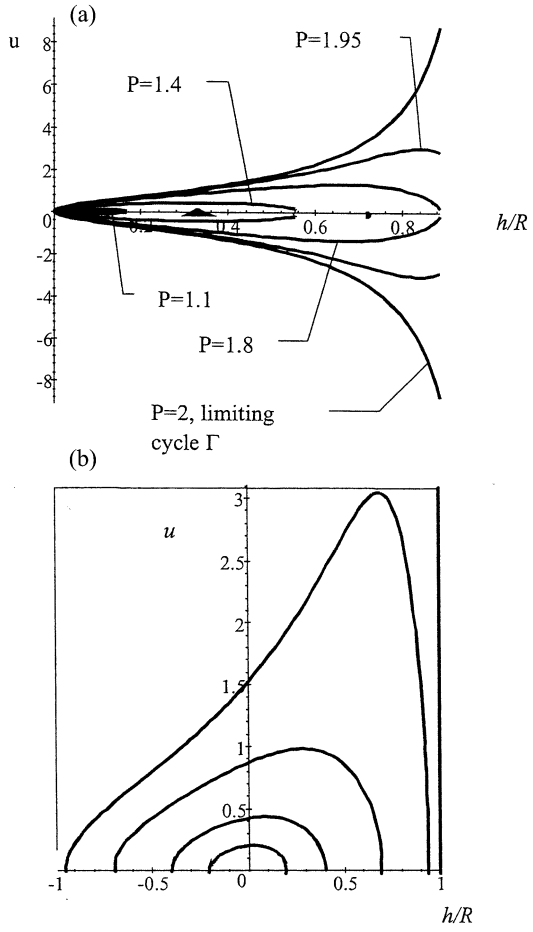

Fig. 3. The case of Laplacian capillarity. (a) When the capillary pressure increases, the integral curve describing the bump is approaching the limiting cycle — meniscus. (b) The upper half of the phase plane, $P_c R/\sigma = 1$.

3.1. Phase portrait

The Laplace equation can be rewritten as the dynamic system:

$$h' = u$$

$$u' = -\frac{(1+u^2)}{(R-h)} + (1+u^2)^{3/2}\ P_c/\sigma. \tag{6}$$

The vector field (h',u') has two singularities (Fig. 3). The singular line $h = R$ reflects the divergence of the Laplacian pressure $\propto 1/(R-h)$ at $h \to R$. The singular point is located on the h-axis and has the abscissa $h = R - \sigma/P_c$. Direct calculations show that the point is elliptic and corresponds to the cylindrical film. The cycles are mathematical images of undulating films. To explore the film morphology, it is convenient to operate with the first integral of Eq. (6):

$$\sigma(R-h)/\sqrt{1+u^2} = \frac{1}{2}P_c(R-h)^2 + C. \tag{7}$$

Here C is a constant. Let us specify the constant by designating the intersection point of the integral curve with the h-axis. This point corresponds to the minimum film thickness H. Denoting the abscissa of the intersection point as H, Eq. (7) can be rewritten in the form:

$$\left(1-\frac{h}{R}\right)/\sqrt{1+u^2} = \frac{P_c R}{\sigma}\left(\frac{H}{R} - \frac{H^2}{2R^2} - \frac{h}{R} + \frac{h^2}{2R^2}\right) + \left(1-\frac{H}{R}\right) \tag{8}$$

Using Eq. (8) we can trace the topological modifications of the integral curves $u(h)$ as the capillary pressure varies.

The case $P_c < 2\sigma/R$. As P_c increases, the elliptic point shifts from the left infinity $h \to -\infty$ to the right, achieving the capillary pressure $P_c = 2\sigma/R$ at the point with the abscissa $h = R/2$. Therewith, the cycles expand from the elliptic point until they reach the limiting cycle, which consists of the integral curve [Eq. (8)], asymptotically merging with the line $h = R$. This limiting cycle can be specified by solving the equation for the abscissa of the intersection point $H = H_{\lim}$

$$\frac{P_c R}{\sigma}\left(\frac{H_{\lim}}{R} - \frac{H_{\lim}^2}{2R^2} - \frac{1}{2}\right) + \left(1 - \frac{H_{\lim}}{R}\right) = 0. \tag{9}$$

A suitable solution for Eq. (9) is $H_{\lim} = R - (2\sigma/P_c)$. A direct calculation shows that the limiting cycle describes a semi-spherical meniscus. $R - H_{\lim}$ is the radius of the capillary that accommodates such a meniscus. As seen from Eq. (8), the limiting cycle branches at infinity from the line $h = R$, $u \to \pm\infty$, and the tangent of the inclination angle at the meniscus cupola behaves as $u \approx \pm(2\sigma/P_c)/(R-h)$.

Outside the limiting cycle, the integral curves form regular streamlines of the

vector field [Eq. (6)] corresponding to nodoids. Indeed, considering the behavior of du/dh in the upper (lower) semi-plane $u > 0$ ($u < 0$), one can be persuaded that the sign of the difference $P_c(R-h)[\sqrt{1+u^2}\,] - \sigma$ specifies the sign of the derivative. Using the first integral [Eq. (7)], we express the difference as $P_c(R-h)[\sqrt{1+u^2}\,] - \sigma = \sigma - 2\sigma C[\sqrt{1+u^2}\,/(R-h)]$. Due to the identity $C = (R-H)(H-H_{\lim})$, the difference is positively definite for any integral curve intersecting the h-axis at $H < H_{\lim}$. Thus, at a given capillary pressure, the minimal thickness of nodoidal films is always smaller than $H_{\lim}$.

A typical phase portrait of Eq. (6) is depicted in Fig. 3. One can imagine a two-dimensional flow produced by a dipole at infinity (with a source at the bottom and a sink at the top). Due to the vortex (elliptic point), the streamlines of the oncoming uniform flow are deformed to avoid the limiting cycle.

The case $P_c = 2\sigma/R$. As the capillary pressure reaches the value $P_c = 2\sigma/R$, the limiting cycle is deformed to pass through the point (0,0). The associated meniscus of radius R meets the capillary wall at zeroth angle (Fig. 3a).

The case $P_c > 2\sigma/R$. For greater capillary pressures, the intersection point $(H_{\lim},0)$ is shifted to the right. Therefore, the radius of associated interface decreases, so that the physical image of the limiting cycle corresponds to a spherical bubble.

3.2. Physical interpretation of solutions

The pressure smaller than σ/R. Physically, the cycles are mathematical images of the undulating films. Only those pieces of the cycles that lie within the strip $0 < h < R$ could serve as suitable solutions of the film profile in a capillary of radius R. Hence, all interface configurations that could be predicted within the Laplacian scheme correspond to exclusive fragments of the complete cycles. All cycles intersect the u-axis whenever the capillary pressure is smaller than σ/R. The solutions correspond to bumps meeting the capillary wall at a non-zeroth contact angle. Thus, no complete wetting occurs in such a case.

Bumps at the condition of complete wetting. Just after the capillary pressure has reached the value σ/R, a uniform wetting film of 'zeroth' thickness first appears as a suitable trivial solution. Increasing the capillary pressure further, we shift to the right the elliptic point together with the set of cycles. Therefore, the uniform film grows to the thickness $h = R - \sigma/P_c$ allowing for the associated undulating film-cycles to oscillate around this value. There is an exceptional cycle Γ that touches the axis $h = 0$ (Fig. 3a). One period of this unduloid describes a solitary bump wetting the capillary wall completely, i.e. for this bump, the boundary condition $u|_{h=0} = 0$ holds. Thus, at equilibrium, the bumps wetting the capillary completely have the capillary pressure, which is always greater than σ/R. Using Eq. (8), we conclude that the height of these bumps varies with the capillary pressure as $h_{\max} = 2R(P_c - \sigma/R)/P_c$.

Bump bridging. When bridging occurs, the bump transforms into a lens spanning the capillary wall. Two semispherical menisci of radius R form this lens. Tracing

the transformations of cycle Γ as the capillary pressure increases, we can elucidate the mathematical mechanism of bump bridging. Namely, it is seen that the bridging occurs due to merging the cycle Γ with the limiting cycle as the capillary pressure increases up to $2\sigma/R$. Thus, the *breaking of symmetry* of the solutions comes out to occur via the bifurcation of unduloid solution.

Foam lamellae. Increasing the capillary pressure above $2\sigma/R$, we displace the set of cycles to the right by deforming the limiting cycle. The limiting cycle for capillary pressures above $2\sigma/R$ is a spherical bubble of radius $R - H_{\text{lim}}$ with the center positioned at the axis of symmetry. The integral curves situated from the left of the limiting cycle describe the nodoidal menisci of bubbles separated by flat freestanding films, e.g. foam lamellae [52,60]. The cusp of the nodoidal meniscus meets the lamella at the height smaller than R.

Undulating films. Undulating films described by a set of cycles inside Γ represent another class of physically reasonable solutions to the Laplace equation. The height of the bump $h_{\max}$ is an upper bound for the elevation of the wave crest for unduloids. Bridging occurs via the same scenario as above, yet the limiting configuration describes a bubble train instead of a solitary lens.

In application to the process of capillary condensation/evaporation, bumps and undulating films are of special interest. The bumps represent key configurations for the case of condensation by nucleation. The undulating films serve as intermediate configurations for the case of condensation in prewetted capillaries.

3.3. Nucleation and bridging, quantitative consideration

Let us consider the process of capillary condensation via the formation of a nucleus in the form of a solitary bump, which grows to create a lens. The dependence characterizing the bridging process is the relation between the bump volume V_{bump} and the capillary pressure P_c. There are two possible processes in which this relation plays a crucial role. Everett and Haynes distinguished two types of equilibrium and stability referred to as Laplace and Kelvin conditions [40]. The Laplace conditions assume the constancy of the liquid volume: a liquid droplet attached to a solid surface takes upon a shape, which minimizes the surface free energy $F_{\text{surf}} = \Sigma\sigma_i A_i$, where σ_i is the surface tension and A_i is the area of separating interfaces. Therefore, the mass exchange between the drop and the environment (vapor phase) is forbidden. The Laplace equilibrium may be unstable in an open system. Stable thermodynamic equilibrium in an open system implies Kelvin conditions, the minimization of the grand thermodynamic potential $\Omega = -P_c V + \Sigma\sigma_i A_i$ with respect to V and A. Ω represents the minimal work of formation of a liquid phase of volume V and interfacial areas A_i at a given P_c. A typical example is a liquid drop in a supersaturated vapor. While the Laplace condition ensures the spherical shape of the drop in an unconfined environment, the Kelvin condition is not fulfilled: the equilibrium drop corresponds to the maximum of the grand thermodynamic potential and represents the work of nucleation. A similar situation is encountered in other nucleation processes, capillary condensation particularly. Physically reasonable for one case (involatile

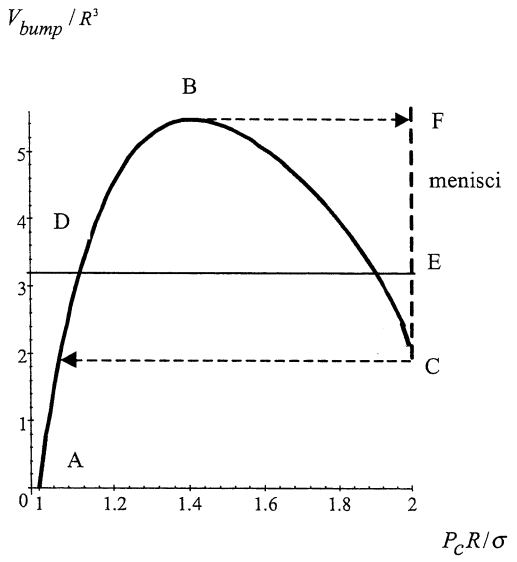

Fig. 4. The bump volume as a function of capillary pressure.

liquid), the scenario of wetting film bridging might be different for another (condensation from a vapor phase).

Volume / pressure relation. Everett and Haynes [40] dealt with the solution presented via elliptic coordinates. We use the first integral [Eq. (8)]. After some algebra, the volume can be expressed via the elliptic integrals $K(k)$ and $E(k)$ as (for details, see [42,61]):

$$V_{\text{bump}} = \pi R^3 \left[\ell - \frac{2(1-H_{\max})^2}{3} \left\{ \left(2 + 3(1-H_{\max})^{-1} + 2(1-H_{\max})^{-2}\right) \times E(k) - K(k) \right\} \right], \tag{10}$$

where

$$\ell = L/R = 2(1-H_{\max}) \left[K(k) + (1-H_{\max})^{-1} K(k) \right]$$

is the dimensionless width of the bump base,

$$k^2 = 2H_{\max} - H_{\max}^2, \text{ and } H_{\max} = h_{\max}/R = 2(P_c - \sigma/R)/P_c$$

is the dimensionless height of the bump. As shown in Fig. 4, the dependence is non-monotonous. In accordance with the Everett and Haynes idea, condensation occurs at the maximum of the function $V_{\text{bump}}(P_c)$.

Thermodynamics of bridging. In their original paper [40], the authors discussed only the Laplace conditions of *volume-controlled transformations*. Therefore, the only surface free energy has been analyzed. The latter is written as, $F_{\text{surf}} = \sigma A_{\text{bump}} + (\sigma_{\text{wet}} - \sigma_{\text{dry}})A_{\text{wet}}$. Here σ_{wet} and σ_{dry} are the surface energies of the liquid/solid and gas/solid interfaces, respectively; A_{bump} and A_{wet} are the surface areas of the vapor/liquid and liquid/solid interfaces. Making use of the condition for complete wetting, $\sigma + \sigma_{\text{wet}} = \sigma_{\text{dry}}$, and the first integral [Eq. (8)], the free energy is transformed to (for details, see [42,61]):

$$F_{\text{surf}} = \sigma(A_{\text{bump}} - A_{\text{wet}}) = 2\pi\sigma R^2\left[2(1 - H_{\max})\left(1 + (1 - H_{\max})^{-1}\right)E(k) - \ell\right] \tag{11}$$

The surface energy (11) is greater for the states on the BC branch compared to the states of the same volume on the AB branch (Fig. 5). Thus, the configurations on the branch BC are unstable. To analyze the conditions of bridging, the bump free energy has to be compared with that of a lens $F_{\text{lens}} = -2\pi\sigma R^2\ell_{\text{lens}}$, where ℓ_{lens} is the dimensionless length of cylindrical liquid column situated between menisci cupolas. The thinnest lens in the limit $\ell_{\text{lens}} \to 0$ transforms into the highest bump $h_{\max} \to R$, point C in Fig. 4. The branch FC in Fig. 5 corresponds to lenses. The surface energy of lenses is smaller than that of bumps of the same volume when the liquid volume exceeds the value corresponded to the intersection point E. The coordinates of point E are specified by the following equation:

$$V_{\text{bump}} = \pi R^3\left(\frac{2}{3} + \ell_{\text{lens}}\right), \quad F_{\text{lens}} = F_{\text{surf}} = -2\pi\sigma R^2\ell_{\text{lens}}.$$

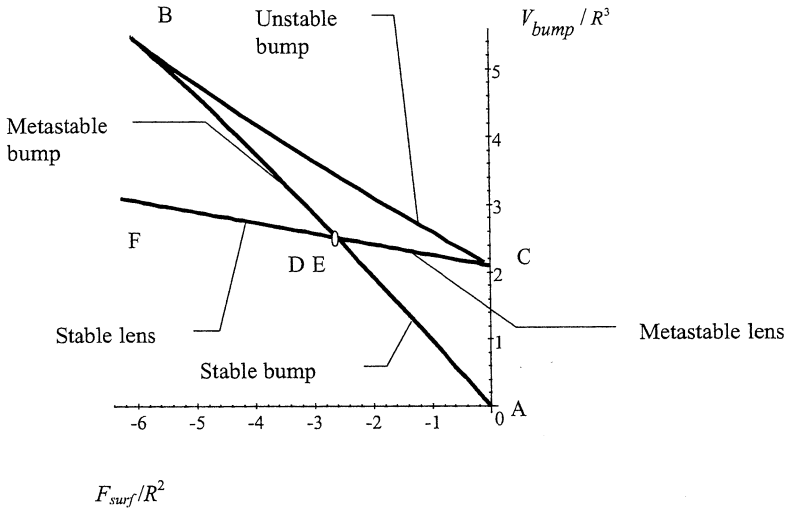

Fig. 5. Surface free energy as a function of bump volume. Points D and E merge.

The configurations along the branches DB and EC are *metastable* [40]. Their surface energy exceeds the surface energy of the stable configurations having the same volume on the branches DF and EA. Nevertheless, if the bump expands due to absorption of the liquid, it snaps off to form a lens as the bump volume reaches point B in Fig. 4. In the process of lens rupturing, the lens disappears just after its volume has descended below point C in Fig. 4.

Nucleation as a pressure-driven transformation. In the process of capillary condensation/evaporation, the increasing branch AB in Fig. 4 is thermodynamically unstable due to the LeChatelier principle: an increase of the capillary pressure must result in decrease of the bump volume. Once appeared, the bump grows up until a bridge forms. Consider an energetic barrier needed for bump formation. Within the above assumptions, the thermodynamic potential can be written as:

$$\Omega = \sigma A_{\text{bump}} + (\sigma_{\text{wet}} - \sigma_{\text{dry}})A_{\text{wet}} + P_c V_{\text{bump}} = \sigma(A_{\text{bump}} - A_{\text{wet}}) + P_c V_{\text{bump}}, \tag{12}$$

where the first term in the RHS is the work taken on formation of the liquid/vapor interface of area A_{bump} and the energy consumed on the wetting of capillary surface of area A_{wet} beneath the bump. The second term is the work taken on displacement of vapor from the bump volume. In Fig. 6, we plot the energy as a function of capillary pressure. The theory predicts that the bumps would appear due to thermal excitations $\Omega \sim kT$. In contrast, the energy gained for creation of a lens is of the order of $\Omega \propto \sigma R^2$, which is much greater than the energy of thermal excitations. For a typical example, we take nitrogen with $\sigma \cong 10^{-2}$ N/m, $T \cong 77$ K

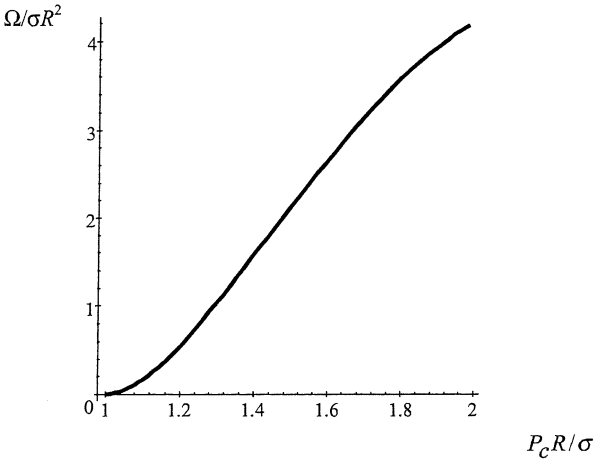

Fig. 6. The energetic barrier as a function of capillary pressure. The bump height and capillary pressure are interconnected by the relation $h_{\max} = 2R(P_c - \sigma/R)/P_c$.

condensing in a pore of 10 nm radius. Lens nucleation requires an energy a few orders of magnitude greater that the energy of elementary excitations.

4. General analysis of the Derjaguin model

For a cylindrical pore, the Derjaguin equation for a non-uniform film of thickness $h(z)$, where z is the axial coordinate, is given by:

$$P_c = \frac{\sigma h''}{(1 + h'^2)^{3/2}} + \frac{\sigma}{(R - h)(1 + h'^2)^{1/2}} + \Pi(h). \tag{13}$$

Due to its non-linearity, Eq. (13) describes a variety of film configurations (see, e.g. the classification of solutions given for van der Waals' films on planar substrates by Neimark and Kornev [52]), which can be analyzed by the methods of dynamic systems. Written as a dynamic system:

$$h' = u$$

$$u' = -\frac{(1 + u^2)}{(R - h)} - (1 + u^2)^{3/2}[-P_c + \Pi(h)]/\sigma. \tag{14}$$

Eq. (14) determines a vector field with components (h,u). The physically meaningful trajectories are confined in the strip $R > h > 0$. As in Section 2 previously, we restrict ourselves to monotonously decreasing disjoining pressure isotherms.

4.1. Stationary points

Within the strip $R > h > 0$, the vector field (h,u) has two stationary points $(h_-,0)$ and $(h_+,0)$ when $P_c > P_{sc}$. The abscissas are the roots of Eq. (1). As noted in Section 2, the stationary points describe *uniform* films. The thinner film of thickness h_- is thermodynamically stable, while the thicker film of thickness h_+ is thermodynamically unstable. Mathematically, the different thermodynamic states of the film are associated with a distinguishing topological pattern of the vector field near the stationary points. In particular, as can be checked by direct calculations, the thinner film corresponds to hyperbolic point and the thicker one is the center for cyclic trajectories. Both solutions merge when the capillary pressure reaches the value P_{sc}. Remarkably, in the limit of the Laplacian capillarity, $\Pi(h) \equiv 0$ there is only one elliptic stationary point associated with the film of thickness h_+.

4.2. Singular lines, or how the wetting film approaches the substrate

The dynamic system [Eq. (14)] has two singular lines, $h = 0$ and $h = R$, forming two borders in the phase plane, Fig. 7. While the latter is the same as in the

Laplacian case, the former is peculiar only for thin films. Recall that in classical capillarity the line $h = 0$ is not singular so that the droplet is allowed to meet the capillary wall by forming any contact angle. However, for films whose disjoining pressure isotherms tend to infinity as the film thickness diminishes, we arrive at a singular behavior of Eq. (14) as h tends to zero. The phase plain construction, therefore, becomes intricate and a local analysis of the system behavior is required.

We consider two physically justified asymptotic forms of the disjoining pressure isotherms, namely, the power kind asymptote $\Pi(h) \propto 1/h^{\eta}$, and the logarithmic asymptote $\Pi(h) \propto -\ln h$ [10,11]. The Frenkel–Halsey–Hill isotherm $\eta = 2.4$, the Hamaker–Lifshitz isotherm, either $\eta = 3$ or $\eta = 4$, or the Derjaguin–Landau isotherms, $\eta = 2$, fall into the former class [9,10]. The 'diffusion cloud' adsorbed onto the substrate can be described by the isotherm with logarithmic singularity. Power type and logarithmic type isotherms result in different behavior of the integral curves at the singular line $h = 0$.

Let us first consider the case of wetting of a planar substrate. For this particular case, we arrive at the equations:

$$\frac{\sigma u}{(1+u^2)^{3/2}}\frac{\mathrm{d}u}{\mathrm{d}h} = P_c - \frac{\alpha_\eta}{h^\eta}, \text{ or } \frac{\sigma u}{(1+u^2)^{3/2}}\frac{\mathrm{d}u}{\mathrm{d}h} = P_c + \beta \ln h. \tag{15}$$

Both equations [Eq. (15)] have the first integrals:

for $\Pi(h) \propto 1/h^{\eta}$:

$$-\frac{\sigma}{(1+u^2)^{1/2}} = P_c h - \frac{\alpha_\eta}{(1-\eta)h^{\eta-1}} + C, \text{ if } \eta \neq 1, \text{ or} \tag{16}$$

$$-\frac{\sigma}{(1+u^2)^{1/2}} = P_c h - \alpha_1 \ln h + C, \text{ if } \eta = 1; \tag{17}$$

for $\Pi \propto -\ln h$:

$$-\frac{\sigma}{(1+u^2)^{1/2}} = P_c h + \beta(h\ln h - h) + C, \tag{18}$$

where C is an integration constant, specific for a given streamline. For the integral curves located near the axis $h = 0$, we can specify the constants by considering the intersection points of the curves with the axis $u = 0$. We denote this point as $h = h_0 \to 0$, $u = 0$. In order to ensure an intersection of the integral curves [Eqs. (16)–(18)] with the u-axis, we have to suppose either $\eta < 1$ for the disjoining

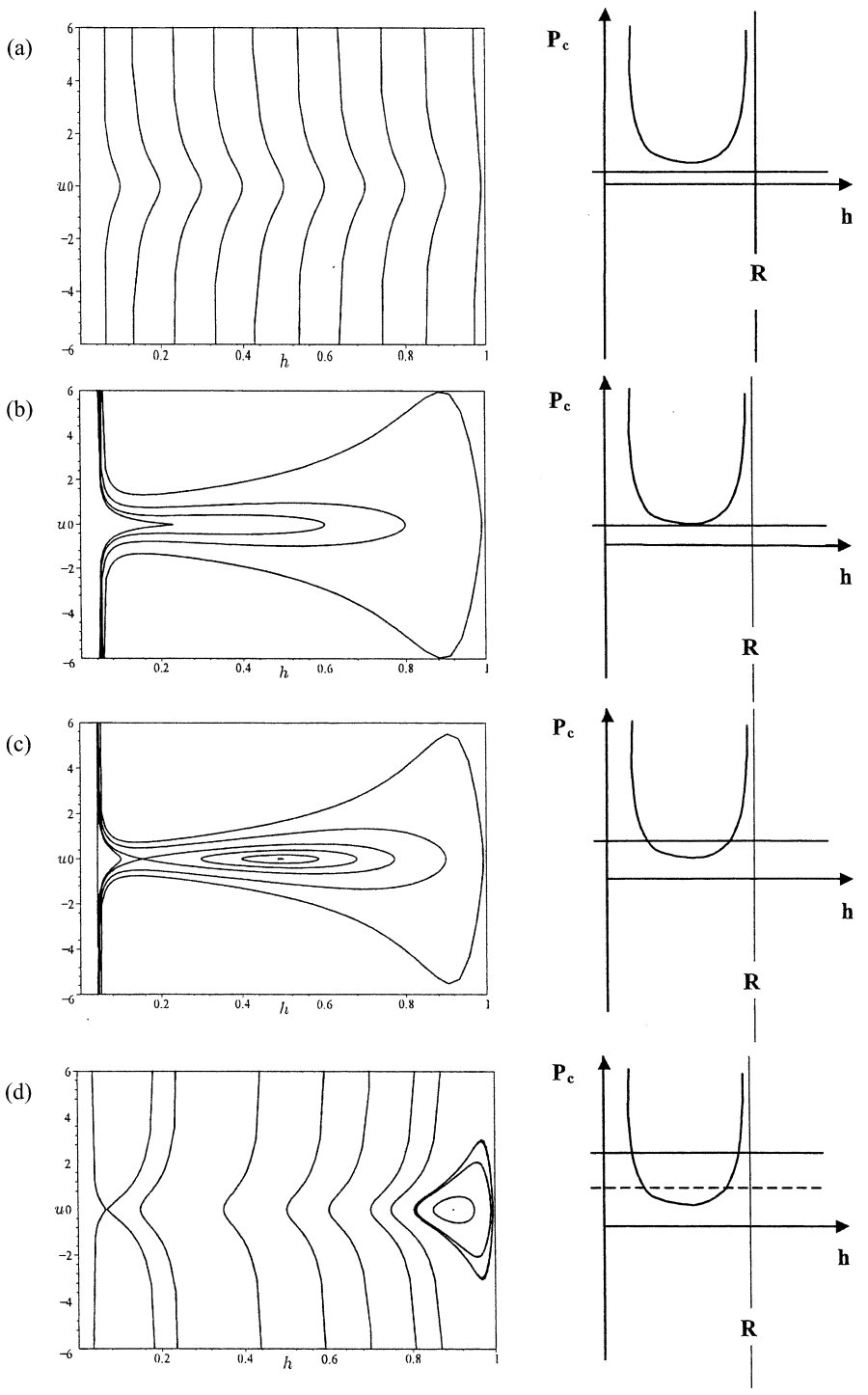

Fig. 7.

pressure isotherms of the form $\Pi(h) \propto 1/h^{\eta}$, or assume that the droplet edge forms a 'diffusive cloud' with the disjoining pressure $\Pi(h) \propto -\ln h$. For both cases, the cosine of the *microscopic contact angle* is $\cos\theta = -C/\sigma$. If, however, the exponent is greater than unity, $\eta \geq 1$, the integral curves [Eqs. (16) and (17)] never intersect the axis $h = 0$ [52]. Emanating from the point $h = h_0 \to 0$, $u = 0$, the curves [Eqs. (16) and (17)], instead of approaching the u-axis, will tend to asymptotes:

$$P_c h - \frac{\alpha_\eta}{(1-\eta)h^{\eta-1}} + C = 0, \text{ if } \eta > 1, \text{ or} \tag{19}$$

$$P_c h - \alpha_1 \ln h + C = 0, \text{ if } \eta = 1. \tag{20}$$

For the integral curves of Eq. (14), the above analysis is also applicable. Indeed, using the first integral of Eq. (14) written as [59]:

$$-\sigma(R-h)/\sqrt{1+u^2} + \sigma(R-h_0) = -\int_h^{h_0}(R-h)(P_c - \Pi(h))dh \tag{21}$$

one can be convinced that the singular terms are captioned asymptotically by Eqs. (16)–(18).

The above analysis tells us that the model with an appropriately chosen disjoining pressure isotherm (finiteness of the integral $\int_0^\infty \Pi dh$ is the necessary condition [51,54]), can be continued to diminishing thickness. However, the isotherm monotonicity causes specific features of the solutions. Namely, the microscopic contact angle cannot be eliminated completely, yet can be made infinitesimally small.

Restricting ourselves to intermediate scales, when the Hamaker–Lifshitz isotherm is suitable, a formal analysis shows that the streamlines of Eq. (14) tend asymptotically to infinity as the film thickness approaches zero [52]. Therewith, the film profile meets the substrate at the right microscopic contact angle. More correctly, just after the film has approached a certain cut-off thickness the solution cannot be continued further. At this point a right angle is formed.

4.3. Separatrices: bumps, edges and menisci

In the case of capillary condensation/evaporation, the capillary pressure has to be considered within the range $P_c > P_{sc}$ (Fig. 2). Just as the capillary pressure

Fig. 7. Typical phase portraits of system (14) for various capillary pressures. (a) The capillary pressure is smaller than the critical level; (b) the capillary pressure achieves the critical level; (c) the capillary pressure ranges from the critical value up to the point of meniscus formation; (d) the capillary pressure is above the point of film/meniscus equilibrium coexistence drawn as the dashed line.

approaches the critical capillary pressure from below, the streamline containing the point $(h_{sc},0)$ deforms to make a cusp at this point (Fig. 7b). The cusp gives birth to two singular points as the pressure increases. Three separatrices separate three distinct streams of the 'phase fluid'. Their two branches emanate from the hyperbolic point and the loop attaches to the hyperbolic point (Fig. 7c).

Edges. The separatrices describe the edges of film continuously transiting into uniform film of thickness h_-. Due to the above analysis, we know that the edges *either meet the dry substrate at a microscopic contact angle* (for isotherms $\Pi(h) \propto 1/h^{\eta}$ with $0 \leq \eta < 1$, and for $\Pi(h) \propto -\ln h$ or are suspended on a cut-off thickness above the wall ($1 \leq \eta$).

Bumps. The loop of separatrix corresponds to a solitary droplet, or bump, which continuously transforms into a uniform film of the equilibrium thickness h_- Fig. 1a).

Menisci. As the capillary pressure increases up to the point P_{sc} (point B in Fig. 2), the loop changes its configuration and merges eventually with the line $h = R$. This limiting cycle corresponds to a meniscus transiting into a uniform film of thickness h_-. In the Laplacian case this moment was absent. There was a limiting cycle, which was moving from the left to the right.

When meeting the cycle Γ, the bump was transforming to a lens. Thus, in the presence of the equilibrium film, the hyperbolic point of Eq. (14), makes the bridging process for ultra thin films distinguishing from the classical case. The breaking of symmetry of solutions happens via creation of a continuous pathway between the hyperbolic point $(h_-,0)$ and infinity (R,∞) (Fig. 1a,b).

Increasing the capillary pressure further, we detach the limiting cycle from the hyperbolic point. As a result, the menisci transiting to the film of thickness h_- change into cusped 'bumps' with a crest height smaller than R. The transformation is seemingly kindred to that we observed in Laplacian case, yet the wetted area is not limited.

4.4. Ribbons and undulating films

Ribbons. Left separatrices emanating from the point $(h_-,0)$ separate two classes of streamlines. The first constitutes the streamlines which lie between the line $h = 0$ and separatrices, while the second class unites the streamlines enveloping the loop of separatrix from the right. Both classes correspond to solitary cylindrical ribbons, which are defined as axisymmetrical films of finite width. In the first class the ribbon height is always smaller than h_-, whenever the height of ribbons of the second class is always greater than the equilibrium film thickness h_-. Both classes of solutions are specific for ultra thin films, because they are associated with the equilibrium film, hyperbolic point of Eq. (14).

Undulating films. Ellipsoidal streamlines or cycles within the loops in Fig. 7c,d correspond to periodic solutions. The situation is analogous to that we observed in the Laplacian case, yet the profile of the corresponding undulated films is different.

4.5. Phase portraits

Using the above results and analyzing the behavior of the derivative du/dh, we can draw four typical phase portraits, depending on the capillary pressure magnitude (Fig. 7a–d). Namely, four ranges of capillary pressure, $P_c < P_{sc}$, $P_c = P_{sc}$, $P_{sc} < P_c < P_{eq}$ and $P_c > P_{eq}$ give distinct phase portraits.

In the first case, $P_c < P_{sc}$, there are no stationary points in Eq. (14), the derivative du/dh is the definite sign in the upper and lower quadrants. Therefore, the streamlines, altogether, look like a uniform flow of a 'phase fluid'; Fig. 7a. Relative to the asymptotic behavior of the disjoining pressure, the streamlines either can or cannot intersect the u-axis. Neither streamline intersects the origin of co-ordinates (0,0). In other words, the macroscopic Derjaguin equation does not allow a droplet of non-volatile liquids to meet a dry substrate at the zeroth microscopic contact angle for any disjoining pressure isotherms with the asymptotic laws, $\Pi(h) \propto l/h^{\eta}$ for $0 \leq \eta < \infty$, and $\Pi(h) \propto -\ln h$.

In three other cases, $P_c = P_{sc}$, $P_{sc} < P_c < P_{eq}$ and $P_c > P_{eq}$; Fig. 7b–d, the streamlines are patterned to form domains in which the topological configurations of the integral curves differ. The physical interpretation of cycles has been presented in Section 3, other configurations associated with the hyperbolic point have been discussed elsewhere for the van der Waals films on planar substrates [52] and we refer the reader to that paper for details.

5. The nucleation theory

In accord with the Everett–Haynes theory for the Laplacian case, we consider that the bumps are nuclei of capillary condensation. The bumps coexist with the films so that the pressure drops in the uniform films and in the bumps are identical. Distinguished from the classical case, the bump has an infinite base wetting film, so that the curvature gradually approaches the value $1/R$. It is instructive to reproduce the Derjaguin equation [Eq. (3)] by following the hypothesis that the bump is an elementary unit of the nucleation theory. In particular, it is able to describe the bridging.

Confirmation of the Derjaguin equations. As follows from the above analysis, the loop-bump first appears at the critical point corresponding to solution of Eqs. (1) and (2) with $\Delta = 0$. Increasing the capillary pressure further, we approach the point $P_c = P_{eq}$; Eq. (4). At this particular capillary pressure, the loop touches the boundary line $h = R$. Consequently, the bump transforms into lens. To check this fact, we consider the first integral of Eq. (14) in its general form [59,60]:

$$-\sigma(R-h)/\sqrt{1+u^2} + \sigma(R-h_{\max})\cos\beta_0 = -\int_h^{h_{\max}} (R-h)(P_c - \Pi(h))dh, \tag{22}$$

where $\cos\beta_0$ is the cosine of the inclination angle at the maximum of the loop, $h = h_{\max}$. The cosine can be either unity, if we deal with the bump, or zero, if we consider a meniscus spanning the capillary walls. However, in the latter case $h_0 = R$. Substituting for the meniscus the appropriate boundary conditions $u = \infty$, $h = R$, and $u = 0$, $h = h_{\text{eq}}$ we reproduce Eqs. (3) and (4). An increase of the capillary pressure above the point $P_c = P_{\text{eq}}$ breaks the bump solution down, as it is seen from Fig. 7d. In other words, the bump is transformed to a meniscus.

Thermodynamics of nucleation. To analyze the nucleation mechanism, let us consider the excess energy needed for bump creation:

$$\Delta\Omega = \Omega_{\text{bump}} - \Omega_{\text{film}} = 2\pi\int_{-\infty}^{\infty}\Big\{\sigma(R-h)[1+h'^2]^{1/2} - \sigma(R-h_{\text{bump}})\Big\}dz$$

$$-2\pi\int_{-\infty}^{\infty}\Bigg\{\int_{h}^{\infty}(R-\xi)\big(P_c(h_{\text{bump}}) - \Pi(\xi)\big)d\xi$$

$$-\int_{h_{\text{bump}}}^{\infty}(R-\xi)\big(P_c(h_{\text{bump}}) - \Pi(\xi)\big)d\xi\Bigg\}dz. \tag{23}$$

The first term on the RHS of Eq. (23) is the excess of surface energy due to surface bending, the second term is the work against film thickening at the bump. $P_c = P_c(h_{\text{bump}})$ is the capillary pressure associated with the equilibrium thickness h_{bump} at infinity. It is worth tracing the analogy with the Laplacian case. Fortunately, there is a small parameter inherent to the Derjaguin model. This parameter allows us to construct an asymptotic theory, the leading term of which is the Laplacian bump. Consider a disjoining pressure isotherm of the form $\Pi = \alpha_\eta/h^\eta$, then the small parameter is $\alpha_\eta/(\sigma R^{\eta-1})$. The Everett–Haynes solution can be proved to be the leading term of asymptotic expansion of the first integral over the parameter $\sqrt[\eta]{\alpha_\eta/(\sigma R^{\eta-1})}$ (see detailed asymptotic analysis of the planar case in [59,60]; for axisymmetric films, the conclusions are similar). As the film thickness is approaching scales of the order of $\sqrt[\eta]{\alpha_\eta/(\sigma R^{\eta-1})}R$, the specific effects of the transition zone come into force. However, the integral characteristics of the solution, e.g. the excess volume relative to the film volume, are given with a high accuracy by the classical model. Therefore, all results that we presented in Section 3 can be treated as asymptotic.

The principal difference between the Laplace and Derjaguin models concerns the immediate vicinity of the critical point $P_c = P_{sc}$, where the solutions to Eq. (14) are singular. This singularity is absent in the Laplacian case. Consequently, the asymptotic analysis fails in this range of capillary pressures. On the other side, namely this region of the phase diagram is responsible for nucleation process. The difficulties can be resolved by using the smallness of the bump amplitude nearly the critical point.

Rewriting Eq. (23) as:

$$\Delta\Omega = \Omega_{\text{bump}} - \Omega_{\text{film}}$$

$$= 2\pi\sigma\int_{-\infty}^{\infty} dz(R-h)\left\{[1+h'^2]^{1/2} - \frac{(R-h_{\text{bump}})}{(R-h)}\right\}$$

$$+2\pi\frac{\sigma}{R-h_{\text{bump}}}\int_{-\infty}^{\infty} dz\int_{h_{\text{bump}}}^{h}(R-\xi)d\xi \qquad > 0$$

$$+2\pi\int_{-\infty}^{\infty} dz\int_{h_{\text{bump}}}^{h}(R-\xi)\big(\Pi(h_{\text{bump}}) - \Pi(h)\big)d\xi \qquad > 0 \tag{24}$$

we can see that the first term is sign $-$ indefinite, while two others are positively definite. In principle, for some disjoining pressure isotherms the first term of Eq. (24) could be balanced by others to achieve the zeroth barrier of bump creation. These expectations, however, have not been confirmed by calculations. We analyzed monotonous disjoining pressures and discovered that the excess energy $\Delta\Omega$ varies as $\propto (h_{\max} - h_{sc})\sqrt{h_{\max} - h_{sc}} > 0$ in the immediate vicinity of the critical point h_∞. The bump amplitude and bump volume at the vicinity of critical point behaves in accordance with the Landau rule [62], $(h_{\max} - h_{sc}) \propto \sqrt{P_c - P_{sc}}$, $(V_{\text{bump}} - V_{\text{film}}^{sc}) \propto \sqrt{P_c - P_{sc}}$. The prefactor is affected by the exponent η, adhesion constant α_η and the capillary radius.

6. Conclusions

Considered as a morphological transition from uniform films to menisci, the problem of capillary condensation has been put into a new frame. An analysis of film patterning has been performed, first, for the classical Laplace theory of capillarity, and then for the Derjaguin model, which takes into account the surface forces expressed in terms of the disjoining pressure. We used the method of dynamic systems to reveal admissible configurations of axisymmetric films coating cylindrical pores. All possible solutions are represented by the streamlines of the phase portrait of the corresponding dynamic system. The mechanisms of the symmetry breaking in film configurations have been elucidated. We trace a pathway of the transformation of an unduloidal bump into a lens spanning the pore cross-section. We show that the energetic barrier of bump formation is smaller that that of lens formation. Moreover, the energy barrier of bump formation decreases to zero as the film thickness approaches the spinodal. In the vicinity of the spinodal, the bumps appear spontaneously due to thermal excitations. Thus, the bump formation is a prerogative of homogeneous nucleation of vapors in confinements.

The Derjaguin model gives rise to distinctive topological patterns of streamlines on the phase portrait. We found a set of admissible solutions to the Derjaguin equation which correspond to different configurations of the liquid–vapor interface in the form of uniform films, solitary bumps, film edges, ribbons, undulating films, menisci of lenses and lamellae, and bubbles. Special attention was paid to the singularities of solutions associated with the divergence of the disjoining pressure isotherms as the film thickness diminishes. We show that the films with integrable monotonous disjoining pressure isotherms form a microscopic contact angle with the substrate. For non-integrable disjoining pressure isotherms, all admissible solutions of the Derjaguin equation imply the right microscopic angle. To state it more correctly, there is a cut-off thickness below which the solution cannot be continued. At the point where the film reaches this thickness, it forms a right angle.

Acknowledgements

This work is partially supported by the TRI/Princeton corporate members. K.G. Kornev and A.V. Neimark thank P.I. Ravikovitch for helpful discussions.

References

[1] B.V. Derjaguin, N.V. Churaev, J. Colloid Interface Sci. 54 (1976) 157.
[2] V.M. Starov, N.V. Churaev, Kolloidn. Zh. 40 (1978) 909.
[3] B.V. Derjaguin, N.V. Churaev, Wetting Films, Nauka, Moscow, 1984.
[4] N.V. Churaev, G. Starke, J. Adolphs, J. Colloid Interface Sci. 221 (2000) 246.
[5] J.C.P. Broechoff, J.H. de Boer, J. Catal. 9 (1967) 8.
[6] J.C.P. Broechoff, J.H. de Boer, J. Catal. 10 (1968) 153.
[7] J.C.P. Broechoff, J.H. de Boer, J. Catal. 10 (1968) 368.
[8] D.H. Everett, in: E.A. Flood (Ed.), The Solid–Gas Interface, 2, Marcel Decker, New York, 1967.
[9] Physical and chemical aspects of adsorbents and catalysts; dedicated to J.H. de Boer on the occasion of his retirement from the Technological University, Delft, The Netherlands. Edited by B.G. Linsen; co-editors J.M.H. Fortuin, C. Okkerse, J.J. Steggerda. Academic Press, London, 1970.
[10] F. Rouquerol, J. Rouquerol, K.S.W. Sing, Adsorption by Powders and Porous Solids: Principles, Methodology and Applications, Academic Press, San Diego, 1999.
[11] B.V. Derjaguin, Acta Physicochim URSS 12 (1940) 181.
[12] W.F. Saam, M.W. Cole, Phys. Rev. B 11 (1975) 1086.
[13] A.V. Neimark, P.I. Ravikovitch, Microporous Mesoporous Mater. 44–45 (2001) 697.
[14] A.V. Neimark, P.I. Ravikovitch, A. Vishnyakov, Phys. Rev. E 62 (2000) R1493.
[15] A.V. Neimark, P.I. Ravikovitch, Stud. Surf. Sci. Catal. 128 (2000) 51.
[16] K. Binder, Ann. Rev. Phys. Chem. 43 (1992) 33.
[17] K. Binder, J. Noneq. Thermodyn. 23 (1998) 1.
[18] A. Vrij, Disc. Faraday Soc. 42 (1966) 23.
[19] E. Ruckenstein, R. Jain, Faraday Trans. 70 (1974) 132.
[20] I.B. Ivanov, D.S. Dimitrov, Colloid Polymer Sci. 252 (1974) 982.
[21] K. Kargupta, R. Konnur, A. Sharma, Langmuir 17 (2001) 1294.
[22] F. Restagno, L. Bocquet, T. Biben, Phys. Rev. Lett. 84 (2000) 2433.

[23] V. Talanquer, D.W. Oxtoby, J. Chem. Phys. 114 (2001) 2793.
[24] K. Lum, A. Luzar, Phys. Rev. E 56 (1997) R6283.
[25] K. Leung, A. Luzar, J. Chem. Phys. 113 (2000) 5836.
[26] K. Leung, A. Luzar, J. Chem. Phys. 113 (2000) 5845.
[27] K. Yasuoka, G.T. Gao, X.C. Zeng, J. Chem. Phys. 112 (2000) 4279.
[28] P.G. Bolhuis, D. Chandler, J. Chem. Phys. 113 (2000) 8154.
[29] W.J. Stroud, J.E. Curry, J.H. Cushman, Langmuir 17 (3) (2001) 688.
[30] A.J. Liu, D.J. Durian, E. Herbolzheimer, S.A. Safran, Phys. Rev. Lett. 65 (1990) 1897.
[31] A.J. Liu, G.S. Grest, Phys. Rev. A 44 (1991) R7894.
[32] M.Y. Lin, S.K. Sinha, J.M. Drake, X.I. Wu, P. Thiyagarajan, H.B. Stanley, Phys. Rev. Lett. 72 (1994) 2207.
[33] L. Monette, A.J. Liu, G.S. Grest, Phys. Rev. A 46 (1992) 7664.
[34] E.V. Albano, K. Binder, D.W. Heermann, W. Paul, Physica A 183 (1992) 130.
[35] S. Puri, K. Binder, J. Stat. Phys. 77 (1994) 145.
[36] M. Meyer, H.E. Stanley, J. Phys. Chem. B 103 (1999) 9728.
[37] L.D. Gelb, K.E. Gubbins, Physica A 244 (1997) 112.
[38] L.D. Gelb, K.E. Gubbins, Phys. Rev. E 55 (1997) R1290.
[39] L.D. Gelb, K.E. Gubbins, Phys. Rev. E 56 (1997) 3185.
[40] D.H. Everett, J.M. Haynes, J. Colloid Interface Sci. 38 (1972) 125.
[41] J.C. Maxwell, Encycl. Brit. 9th Ed., Vol 5 (1875), p. 56.
[42] H.M. Princen, in: E. Matijevic (Ed.), Surface and Colloid Science, 2, John Wiley & Sons, New York, 1969, p. 1.
[43] D.H. Michael, Ann. Rev. Fluid Mech. 13 (1981) 189.
[44] B.J. Lowry, P.H. Steen, Proc. R. Soc. London, A 449 (1995) 411.
[45] P. Kralchevsky, K. Nagayama, Particles at Fluid Interfaces and Membranes, Elsevier, New York, 2001.
[46] K. Rejmer, S. Dietrich, M. Napiorkowski, Phys. Rev. E 60 (1999) 4027.
[47] P.G. de Gennes, Rev. Mod. Phys. 57 (1985) 827.
[48] J.F. Joanny, J. Mech. Theor. Appl. (Paris), Numero special, 249 (1986).
[49] F. Brochard, J. Chem. Phys. 84 (1986) 4664.
[50] F. Brochard-Wyart, J.M. di Meglio, D. Quere, P.G. de Gennes, Langmuir 7 (1991) 335.
[51] V.M. Starov, Adv. Colloid Interface Sci. 39 (1992) 147.
[52] A.V. Neimark, K.G. Kornev, Langmuir 16 (2000) 5526.
[53] E. Ruckenstein, P.S. Lee, Surf. Sci. 52 (1975) 298.
[54] G.J. Hirasaki, J. Adhes. Sci. Technol. 7 (1993) 285.
[55] E.K. Yeh, J. Newman, C.J. Radke, Colloids Surf. A 156 (1999) 137.
[56] E.K. Yeh, J. Newman, C.J. Radke, Colloids Surf. A 156 (1999) 525.
[57] Yu. Solomentsev, L.R. White, J. Colloid Interface Sci. 218 (1999) 122.
[58] J.R. Philip, J. Chem. Phys. 66 (1977) 5069.
[59] A.V. Neimark, L.I. Kheifetz, Kolloidn. Zh. USSR 43 (1981) 500.
[60] K. Kornev, G. Shugai, Phys. Rev. E 58 (1998) 7606.
[61] B.J. Carroll, J. Colloid Interface Sci. 57 (1976) 488.
[62] L.D. Landau, E.M. Lifshitz, Statistical Mechanics, Nauka, Moscow, 1995.